Direct control of fractal pattern generation on an optical fractal synthesizer

Toru Sasaki, Jun Tanida, and Yoshiki Ichioka

We propose a method for direct control of position, rotation, and scaling of fractal patterns generated on an optical fractal synthesizer. In this method we introduce an iterated-function-system mother function to produce control parameters for arbitrary fractal patterns. We implemented the method experimentally and verified the effectiveness of the method. © 2000 Optical Society of America

OCIS codes: 100.1160, 200.3050, 200.4960.

1. Introduction

Fractal geometry has been widely studied in various research fields including image processing and data compression.[1–3] Among the various fractal geometry techniques, a fractal image coding technique is promising because of its potential capability for high compression ratio.[3–6] Although the fractal image coding and decoding techniques require extensive computation in image rotation and pattern matching, optical implementations can provide excellent processing capabilities.

We have presented an optical fractal synthesizer (OFS), which generates a fractal pattern by use of a television feedback system.[7] The shape of the generated fractals are specified by the system parameters of the OFS. One of the problems in this method is difficulty in controlling the status of rotation, scaling, and positioning of the pattern, because these properties do not appear explicitly in the parameter set of an iterated function system (IFS).[3]

In this paper we introduce an IFS mother function to solve the problem. The IFS mother function contains control variables for rotation, scaling, and positioning and produces parameter sets for the IFS. By specifying the variables, we can obtain the IFS corresponding to the property and generate the fractal with the IFS. Section 2 describes the IFS and the OFS and clarifies their relation. Section 3 explains details of the IFS mother function. Section 4 shows the results of an optical experiment for verification of the proposed method.

2. Iterated Function System and Optical Fractal Synthesizer

The IFS is defined as a function system consisting of multiple contractive transformations on a metric space.[3] As an example, an IFS composed of contractive affine transformations is described by Eq. (1),

$$W(A) = \bigcup_{i=1}^{N} w_i(A), \qquad A \subset \mathbf{R}^2, \tag{1}$$

where A is a set of points in a two-dimensional plane $\mathbf{R}^2$. Note that the set A describes a two-dimensional pattern. $w_i(A)$ is a contractive affine transform of A defined as follows:

$$w_i(A) = \left\{ \mathbf{x}'; \mathbf{x}' = \begin{bmatrix} a_i & b_i \\ c_i & d_i \end{bmatrix} \mathbf{x} + \begin{pmatrix} e_i \\ f_i \end{pmatrix}, \mathbf{x} \in A \right\}, \tag{2}$$

where $\mathbf{x}$ and $\mathbf{x}'$ are two-dimensional vectors and $|a_i d_i - b_i c_i| < 1$. If the IFS is applied to a set of points iteratively, the following relation is obtained,

$$B_{n+1} = W(B_n), \qquad B_n \subset \mathbf{R}^2, \tag{3}$$

where n is an iteration number. A stable set of points is obtained after a sufficient number of iterations as follows:

$$B_\infty = W(B_\infty), \qquad B_\infty \subset \mathbf{R}^2. \tag{4}$$

The stable set of points B_∞ is called an attractor of W, which represents a fractal pattern. The shape of the attractor is determined by the coefficient set

The authors are with Department of Material and Life Science, Graduate School of Engineering, Osaka University, 2–1 Yamadaoka, Suita, Osaka 565-0871, Japan. T. Sasaki's e-mail address is sasaki@redeye.ap.eng.osaka-u.ac.jp.

Received 8 March 1999; revised manuscript received July 12 1999.

0003-6935/00/172959-06$15.00/0

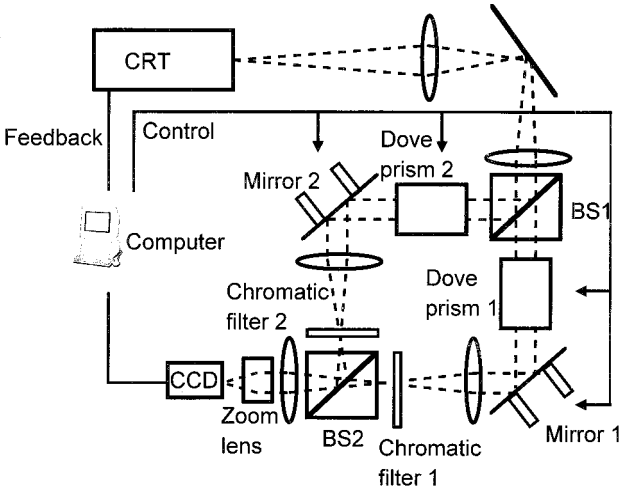

Fig. 1. Schematic diagram of experimental OFS.

$\{a_i, \ldots, f_i\}$ in Eq. (2). The coefficients are called IFS codes.

The OFS archives the contractive affine transformations of the IFS by optical transforms, i.e., reflection, rotation, scaling, and translation. Figure 1 shows a schematic diagram of the experimental OFS. This system can generate the attractor for given IFS codes by optical feedback processing. The input image is displayed on the CRT and duplicated by the beam splitter BS1. Each image is rotated and reflected by the dove prism and translated by the tilted mirror in the optical path. The images passing through the different paths are combined by the beam splitter BS2. After scale reduction by the zoom lens, the resultant image is captured by the CCD camera.

Figure 2 shows an example of fractal pattern generation by the experimental OFS. By the iterative transformation for the initial rectangle pattern A_0, the pattern sequence A_n ($n = 1, 2, \ldots, 8$) is obtained. After the sixth iteration, the fractal shape is not changed, owing to the finite pixel size of the system.

When a set of the bright points in the input image are defined as A, the optical transform is represented as Eq. (5),

$$w_i(A) = \{\mathbf{x}'; \mathbf{x} = S(s_i)R(\theta_i)M(j_i)\mathbf{x} + \mathbf{t}_i, \mathbf{x} \in A\} \quad (i = 1, 2), \tag{5}$$

where s_i is a reduction ratio, θ_i is a rotation angle, j_i is a reflection parameter (-1 for reflection and 1 for no reflection), and $\mathbf{t}_i$ is a vector for translation. $S(s)$, $R(\theta)$, and $M(j)$ are scaling, rotation, and reflection operators shown in following equations:

$$S(s) = \begin{bmatrix} s & 0 \\ 0 & s \end{bmatrix}, \tag{6}$$

$$R(\theta) = \begin{bmatrix} \cos\theta & -\sin\theta \\ \sin\theta & \cos\theta \end{bmatrix}, \tag{7}$$

$$M(j) = \begin{bmatrix} j & 0 \\ 0 & 1 \end{bmatrix}, \qquad j \in \{1, -1\}. \tag{8}$$

With feedback of the captured image into the CRT the iterative processing shown in Eq. (3) is achieved. As

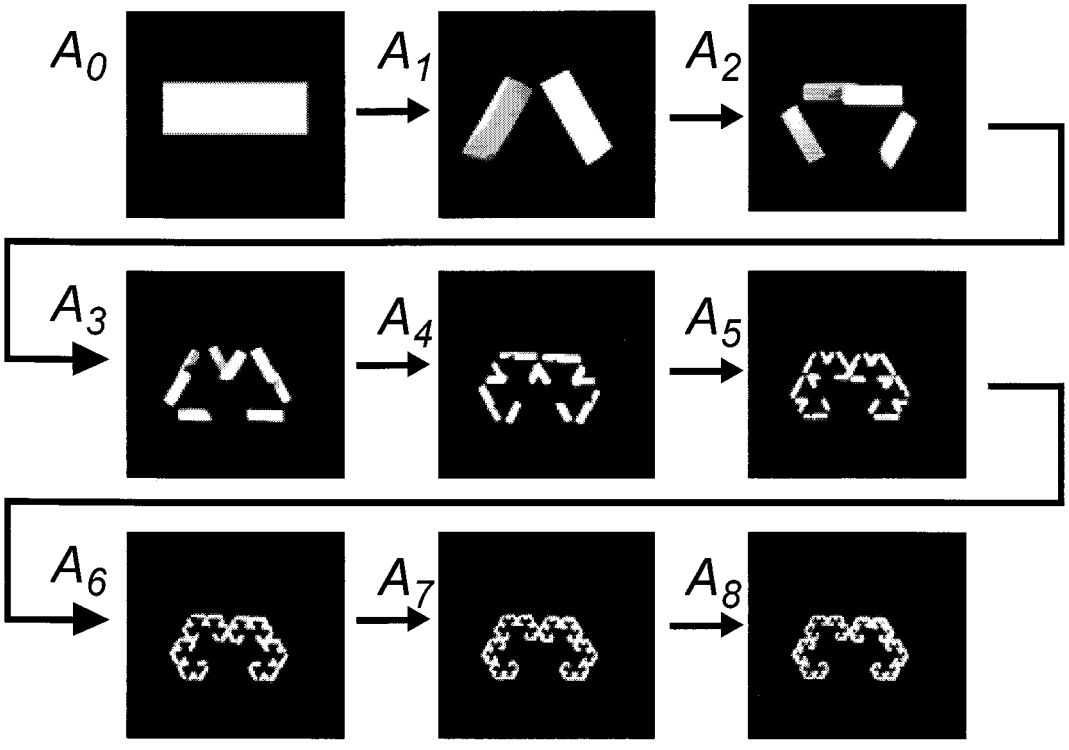

Fig. 2. Time evolution of generated pattern on experimental OFS.

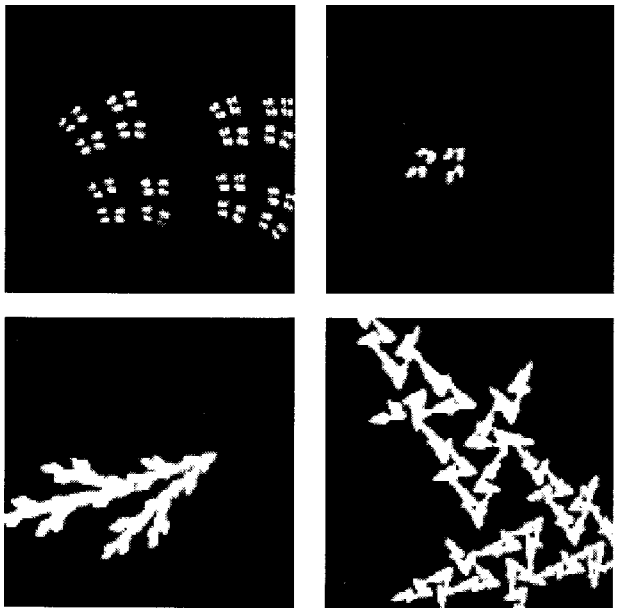

Fig. 3. Attractors generated by experimental OFS.

a result we can generate the attractor by the iterative transformation.

Figure 3 shows examples of the fractal patterns generated by the experimental OFS. We can generate various patterns, whose shape, scaling, and position are different from one another. A problem of the system is difficulty in controlling the pattern with the geometrical properties, such as rotation, scaling, and position, because these parameters do not appear explicitly in the IFS codes.

A digital computer can generate fractal patterns with arbitrary resolution according to the same algorithm as the OFS. However, implementation by the digital computer requires long computational time, because affine transformations must be executed for each pixel, and the same calculation must be iterated. The minimum iteration number required for the fractal pattern generation is determined by the resolution of the image plane and the maximum scaling ratio of the affine transformations with the following relationship:

$$s^i \leq 1/k, \tag{9}$$

where s is the maximum scaling ratio in the set of affine transformations, i is the iteration number, and the image plane consists of $k \times k$ pixels. With the iteration number i satisfying relation (9), arbitrary initial patterns are transformed into an identical fractal shape on a $k \times k$ pixel image plane. For $s = 0.6$ and $k = 256$ the iteration number should not be less than 11. In the case of two affine transformations, $256 \times 256 \times 11 \times 2$ of affine transformations must be executed for each iteration. Although a random iteration algorithm[5] can be applied to reduce computational complexity, a large amount of calculation is still required for large k.

For the OFS, resolution of the generated fractal patterns is restricted by the CRT and the CCD camera. However, our implementation has scalability in the pixel number of the image, which enables us to reflect progress in optoelectronic devices directly to improve processing performance.

3. Iterated-Function-System Mother Function

The IFS mother function is defined by

$$w_i(A) = \{\mathbf{x}'; \quad \mathbf{x}' = \mathcal{B}\mathcal{A}_i\mathcal{B}^{-1}(\mathbf{x} - \mathbf{b}) + \mathcal{B}\mathbf{a}_i + \mathbf{b}, \quad \mathbf{x} \in A\}, \tag{10}$$

where $\mathcal{A}_i$ is a two-dimensional matrix with $|\det \mathcal{A}_i| < 1$ and $\mathcal{B}$ is a two-dimensional matrix with $|\det \mathcal{B}| \neq 0$. Here det represents a determinant of a matrix. $\mathbf{a}_i$ and $\mathbf{b}$ are two-dimensional vectors. $\mathcal{B}^{-1}$ is an inverse matrix of $\mathcal{B}$. When we configure these matrices and vectors $\{\mathcal{A}_i, \mathbf{a}_i, \mathcal{B}, \mathbf{b}\}$, the IFS is specified. $\{\mathcal{A}_i, \mathbf{a}_i\}$ determines the shape of the attractor for the specified IFS. $\mathcal{B}$ denotes the deformation properties of the attractor, such as rotation and scaling. $\mathbf{b}$ represents the position of the attractor.

When $\mathcal{B}$ is a unit matrix and $\mathbf{b} = 0$, Eq. (10) is rewritten as follows:

$$u_i(A) = \{\mathbf{x}'; \quad \mathbf{x}' = \mathcal{A}_i\mathbf{x} + \mathbf{a}_i, \quad \mathbf{x} \in A\}. \tag{11}$$

We call the attractor for Eq. (11) the standard attractor. Derivation of Eq. (10) is described in Appendix A.

For applying to the OFS, the matrix term $\mathcal{B}\mathcal{A}_i\mathcal{B}^{-1}$ in Eq. (10) should be written as a product of the reflection, rotation, and scaling operators that are described in Eqs. (6)–(8). To satisfy the requirement, $\mathcal{A}_i$ and $\mathcal{B}$ are represented as the following equations:

$$\mathcal{A}_i = S(s_i)R(\theta_i)M(j_i), \tag{12}$$

$$\mathcal{B} = S(s_a)R(\theta_a)M(j_a), \tag{13}$$

where s_i and s_a are reduction ratios, θ_i and θ_a are rotation angles, and j_i and j_a are reflection parameters. Consequently, Eq. (10) is rewritten as follows,

$$w_i(A) = \{\mathbf{x}'; \mathbf{x}' = R(\theta_a)M(j_a)S(s_i)R(\theta_i)M(j_i)M(j_a) \times R(-\theta_a)(\mathbf{x} - \mathbf{t}_a) + S(s_a)R(\theta_a)M(j_a)\mathbf{t}_i + \mathbf{t}_a, \quad \mathbf{x} \in A\}, \tag{14}$$

where $\mathbf{t}_i$ and $\mathbf{t}_a$ are vectors for translation. The parameter set $\{s_i, \theta_i, j_i, \mathbf{t}_i\}$ is used to generate a standard attractor. The parameter set $\{s_a, \theta_a, j_a, \mathbf{t}_a\}$, whose members are called manipulating parameters, is used to manipulate the scale, rotation, reflection, and translation of the standard attractor. Configuring these parameters, we can generate the IFS for the fractal with the desired scale, rotation, reflection, and position.

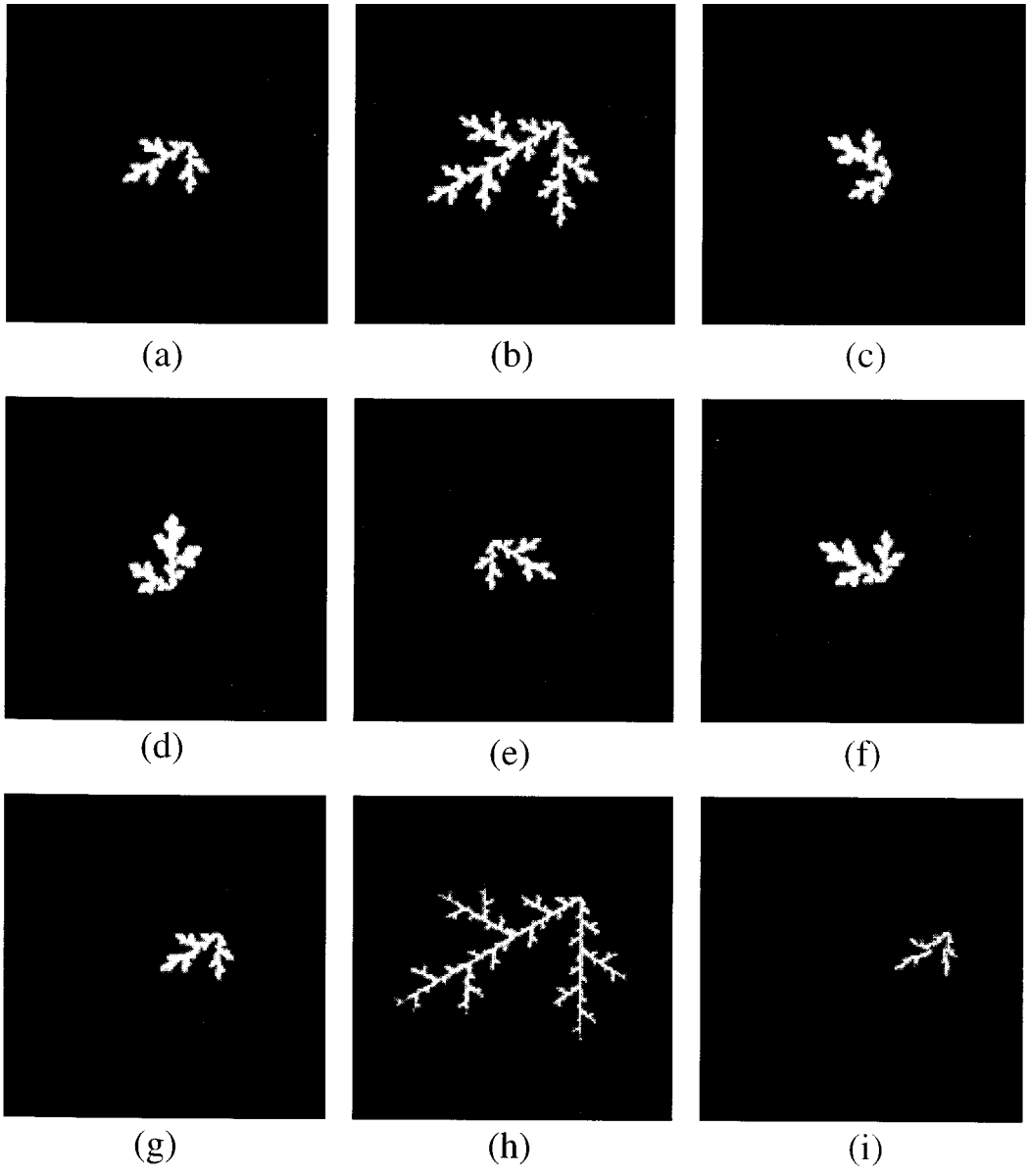

Fig. 4. (a) Standard attractor. (b)–(i) Several variations in position, rotation, reflection, and scaling. Tables 1 and 2 summarize parameters to control the patterns.

4. Experimental Verification and Application

To verify the proposed method, we applied it to fractal generation on the experimental OFS. The image size of the system is 512 × 512 pixels. On the experimental OFS an image captured by the CCD camera is transferred to the computer and some operations are applied, such as intensity binarization and equalizing the image plane. In the experiment, the intensity of each pixel of the captured image is binarized by a thresholding operation to simplify the generated fractal pattern. Equalization is not executed, because of good intensity uniformity on the

Table 1. Parameter Sets for Standard Attractor Used in Experimental Verification

i	s_i	θ_i	j_i	$\mathbf{t}_i$
1	0.65	60	−1	(30, 0)
2	0.65	120	−1	(−30, 0)

Table 2. Manipulating Parameters Used in Experimental Verification

Pattern	s_a	θ_a	j_a	$\mathbf{t}_a$
(a)	1.0	0	1	(0, 0)
(b)	2.0	0	1	(0, 0)
(c)	1.0	60	1	(0, 0)
(d)	1.0	120	1	(0, 0)
(e)	1.0	0	−1	(0, 0)
(f)	1.0	180	−1	(0, 0)
(g)	1.0	0	1	(50, 0)
(h)	3.0	0	1	(0, 0)
(i)	1.0	0	1	(100, 0)

image plane. Determination of the threshold is an important problem, because a fractal pattern cannot be generated for high threshold, whereas resolution of the pattern is reduced for low threshold. In this experiment we adjust the threshold manually to obtain the fractal pattern with high resolution.

The IFS codes are precisely set with the three-point method.[8] This method is achieved by the following procedure:

1. Display a bright point on the CRT at a position. The point is duplicated by the beam splitter and passes through the optical paths.
2. Capture the duplicated points by the color CCD camera, and identify the point for each optical path. The color CCD camera can identify the path by the color associated with the chromatic filter. As a result, positions of the transformed points passing through each optical path are obtained.
3. Repeat steps 1 and 2 three times with display of a bright point at different positions.
4. Calculate the IFS codes for each optical path by the positions obtained in the above steps. This calculation is described by a simple simultaneous equation.[8]
5. Adjust the actuators of the optical setup to compensate difference between the target and the obtained IFS codes.

Repeating the above procedures, we can configure the system with high precision.

To investigate the effectiveness of the proposed pattern-control method, a standard attractor and several variations in position, rotation, reflection, and scaling were generated as shown in Fig. 4. The parameter sets $\{s_i, \theta_i, j_i, \mathbf{t}_i\}$ for the standard attractor are shown in Table 1. The manipulating parameters $\{s_a, \theta_a, j_a, \mathbf{t}_a\}$ for these fractal generations are shown in Table 2. As seen from Figs. 4(b)–4(g), the desired shapes are correctly obtained. Note that Fig. 4(b) has finer structure than the standard pattern. This fact shows that, although the minimum size of the pattern structure is limited by the optical system, we can retrieve the fine structure by using a transformation with magnification.

Figures 4(h) and 4(i) show examples of unexpected patterns. They are expected to have the same shapes as the pattern of Fig. 4(a) and to be magnified $3\times$ or translated by 100 pixels to the right-hand side. As seen from the figures, these patterns have thinner structure and are different from the expected shapes. The reason for the unexpected pattern generation is the finite size of the image planes of the OFS. In the case of Figs. 4(h) and 4(i), some bright points on the CRT are not captured by the CCD camera, owing to large value of the translation terms of the affine transformations.

Figure 5 shows the relationship between the translation vector $\mathbf{k}_i$ and the captured area. For simplicity, the large circle denotes the area captured by the CCD, and the shaded circle represents the bright point set on the CRT which is mapped by the affine transformation. If the shaded circle is included in the large circle, all points on the CRT are captured by the CCD. Therefore, if the translation vector $\mathbf{k}_i$ satisfies the following equation, all points are captured, and the desired fractal pattern can be obtained,

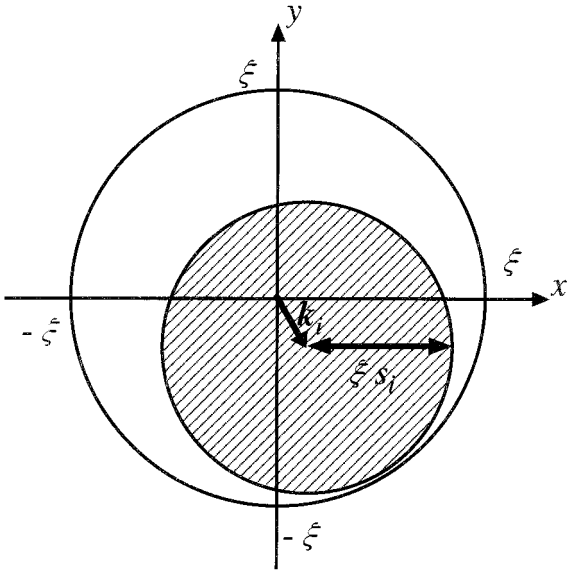

Fig. 5. Relationship between translation vector of affine transform and captured area.

$$\xi > \xi s_i + |\mathbf{k}_i|, \tag{15}$$

where ξ is the radius of the captured area, which is 256 for the experimental OFS. s_i is the scaling parameter of each affine transformation. In this experiment, s_1 and s_2 are 0.65. From relation (15), if $|\mathbf{k}_i|$ is smaller than 89.6, the desired fractal pattern can be obtained. In the cases of Figs. 4(h) and 4(i) the translation vectors are (90, 0) and (−90, 0) for (h) and (160, 52) and (40, 52) for (i). The absolute values of these vectors are 90 for (i) and 168 and 66 for (h). These values do not satisfy relation (15), so the unexpected shape is generated.

As an application of the method we consider image encoding by the IFS codes. In this technique, similarity between a target image and a fractal pattern generated by the OFS is evaluated. To find the IFS codes corresponding to the target, the same process is repeated with a change of parameters for generation. Although this algorithm is still indirect, controllability in fractal generation by the proposed method is expected to increase processing efficiency and processing speed.

5. Conclusion

We have proposed a method to control fractal pattern generation on the basis of the IFS mother function. By means of the experimental OFS we have investigated the effectiveness of the proposed method. Most of the example patterns are correctly controlled, but some undesired patterns are also observed. As a reason for the undesired pattern generation we have shown the finite size of the image plane of the OFS.

This method is expected to be used for a fractal image encoding technique.

Appendix A: Derivation of Iterated-Function-System Mother Function

The IFS mother function is derived from the IFS of the standard attractor and the conversion on the standard attractor. The IFS of the standard attractor is written as follows:

$$U(A) = \bigcup_{i=1}^{N} u_i(A), \qquad A \subset \mathbf{R}^2, \tag{A1}$$

where $u_i(A)$ is the affine transformation for the standard attractor described in Eq. (11). The standard attractor is represented as a point set α satisfying the following equation:

$$\alpha = U(\alpha), \qquad \alpha \subset \mathbf{R}^2. \tag{A2}$$

If the target attractor of the control is represented by β, β satisfies the subsequent equation

$$\beta = v(\alpha), \tag{A3}$$

where v is the affine transformation for conversion onto the standard attractor described as follows,

$$v(A) = \{\mathbf{x}'; \quad \mathbf{x}' = \mathcal{B}\mathbf{x} + b, \quad \mathbf{x} \in A\}, \tag{A4}$$

where $\mathcal{B}$ and $\mathbf{b}$ correspond to Eq. (10). From Eqs. (A2) and (A3) the following equation is derived,

$$\beta = v\{U[v^{\text{inv}}(\beta)]\} = \bigcup_{i=1}^{N} v\{u_i[v^{\text{inv}}(\beta)]\}, \tag{A5}$$

where v^{inv} is the inverse transformation of v described as follows:

$$v^{\text{inv}}(A) = \{\mathbf{x}'; \quad \mathbf{x}' = \mathcal{B}^{-1}(\mathbf{x} - \mathbf{b}), \quad \mathbf{x} \in A\}. \tag{A6}$$

Equation (A5) shows that the point set β is an attractor of the IFS composed of the following affine transformations:

$$w_i(A) = v\{u_i[v^{\text{inv}}(\beta)]\} = \{\mathbf{x}'; \quad \mathbf{x}' = \mathcal{B}\mathcal{A}_i\mathcal{B}^{-1}(\mathbf{x} - \mathbf{b}) + \mathcal{B}a_i + \mathbf{b}, \quad \mathbf{x} \in A\}. \tag{A7}$$

These affine transformations are the same as Eq. (10), and derivation is finished.

References

1. B. B. Mandelbrot, *The Fractal Geometry Of Nature* (Freeman, New York, 1977).
2. H. Peitgen, H. Jürgens, and D. Saupe, *Chaos and Fractals* (Springer-Verlag, New York, 1992).
3. M. Barnsley, *Fractals Everywhere* (Academic, San Diego, Calif., 1988).
4. A. Jacquin, "Image coding based on a fractal theory of iterated contractive image transformation," IEEE Trans. Image Process. **1,** 18–30 (1992).
5. N. Lu, *Fractal Imaging* (Academic, San Diego, 1997).
6. G. Held and T. R. Marshall, *Data and Image Compression* (Wiley, Chichester, UK, 1996).
7. J. Tanida, A. Uemoto, and Y. Ichioka, "Optical fractal synthesizer: concept and experimental verification," Appl. Opt. **32,** 653–658 (1993).
8. T. Sasaki, J. Tanida, and Y. Ichioka, "Optical implementation of high-accuracy computing based on interval arithmetic and fixed point theorem," Opt. Eng. **38,** 508–513 (1999).